# DESIGN AND CONTROL FOR RECYCLE PROCESS WITH TUBULAR REACTOR

**Yih-Hang Chen[1] and Cheng-Ching Yu[2*]**

*Department of Chemical Engineering[1]*

*National Taiwan University of Science and Technology Taipei 106-07, TAIWAN*

*Department of Chemical Engineering[2]*

*National Taiwan University Taipei 106-17, TAIWAN*

**Abstract:** Interaction between design and control for gas-phase adiabatic tubular reactor with liquid recycle is studied. This generic bimolecular reaction, $\mathcal{A}+\mathcal{B}\rightarrow\mathcal{C}$, has two important features: (1) stoichimoetiric balance has to be maintained and (2) reactor temperature plays an important role in design and operability. More importantly, it represents a large class of important industrial processes. Optimal reactant distribution can be obtained directly form the simplified TAC equation and effects of kinetics parameters and relative volatilities on this optimality are also explored. The results show that an increased reactor exit temperature leads to a more controllable optimal design while a high activation energy results in a less controllable one. For the operability analysis, two control structures are proposed with three different combinations of TPM. The control structure using the reactor inlet temperature as TPM gives good control performance when the reactant distribution is held constant. However, potential problem may arise as the result of high reactor exit temperature ($T_{out}$). For the case of biased reactant distribution, the reactant redistribution provides an extra degree of freedom and this alleviates the high $T_{out}$ problem. The results presented in this work clearly indicate that simple material and energy balances provide useful insights in the design and control of recycle processes.

*Keywords***:** recycle process, plantwide control, interaction between design and control, tubular reactor.

## 1. INTRODUCTION

Buckley's pioneer work on the plantwide control has been widely adopted in industry for many years. The first step is to lay the "material balance" control structure that handles the inventory controls. Then "product quality" loops are closed on each of the individual units. Since these loops are typically much faster than the slow inventory loops, interaction between the two is often not a problem. Steady development on the dynamics and control of recycle processes is also witnessed from 60s to 80s as can be seen in Gilliland et al. [1], Verykios and Luyben [2], and references therein. Unfortunately, progress in plantwide control is hindered by the lack of software support. During that incubation period, conceptual plantwide control design procedure is formulated, but it was difficult to validate such design procedures except for limited cases (as a result of extensive engineering manpower required for modeling and simulation). In early 90s, the increased computing power and the advent of dynamic process simulators, such as HYSYS and Aspen Dynamics, lead to renewed engineering practice.

Subsequent plantwide control research can be divided into two schools. One group tends to provide fundamental understanding of the problem [3, 4, 5].

Another group tried to provide a systematic procedure for the design of plantwide control system[6, 7, 8]. Most of the above mentioned literature addresses the control issues. Much less work has been done on the interaction between design and control. Elliott and Luyben [9] evaluate the steady-state design of a ternary system based on the total annual cost (TAC) and controllability is assessed quantitatively using capacity-based approach evaluate different designs using several control measures, e.g., relative gain array, and relative disturbance gain. These approaches akin to a sequential control-design approach. That is controllability analysis is an add-on feature to a design problem. Luyben et al. [10] analyze the pole location of a ternary system using simple dynamic reactor model and this provides an insight into potential control problem with any given design. Chen and Yu [11, 12] extend such approach to the design of feed-effluent heat exchangers, heat-integrated reactors. Cheng and Yu [13] proposed a framework for analyzing design and control simultaneously. Ternary systems with a bimolecular reaction ($\mathcal{A}+\mathcal{B}\rightarrow\mathcal{C}$) in a CSTR and separators were studied and possible tradeoffs between design and control were explored. The objective of this work is to extend the approach of Cheng and Yu [13] to systems with simultaneous material and energy recycles.

## 2. STEADY-STATE DESIGN

### *2.1 Process*

Consider a recycle process where an irreversible, exothermic reaction $\mathcal{A}+\mathcal{B}\rightarrow\mathcal{C}$ occurs in a gas phase, adiabatic tubular reactor. The process flowsheet consists of one tubular reactor, one distillation column, one vaporizer, and one furnace with two heat exchangers which was first studied by Reyes and Luyben [14] (Fig. 1). Two fresh feed streams $F_{0A}$and $F_{0B}$ are mixed with the liquid recycle stream D and sent to a steam-heated vaporizer. According to the requirement of reaction temperature, the vapor from the vaporizer outlet stream is preheated first in a feed-effluent heat exchanger followed by a furnace to get proper reactor temperature as well as for the start-up purpose. The exothermic reaction takes place

in the tubular reactor and the reactor temperature increases monotonically along the axial direction with the following inlet and outlet temperatures, $T_{in}$ and $T_{out}$. The hot gas from the reactor preheats the reactor feed in a feed-effluent heat exchanger, HX1, and the liquid recycle stream in a second heat exchanger, HX2, as shown in Fig. 1.

After heat recovery, via HX1 and HX2, the reactor effluent is fed into a distillation column. The two reactants, A & B, are light key (LK) and intermediate boiler (IK), respectively, while the product, $\mathcal{C}$, is the heavy component (HK). The Antoine constants of the vapor pressure equation are chosen such that the relative volatilities of the components are $\alpha_A = 4$, $\alpha_B = 2$, and $\alpha_C = 1$ for this equal molar overflow system (Table 1). Only one distillation column is sufficient to separate the product (C) from the unreacted reactants ($\mathcal{A}$ & $\mathcal{B}$). Ideal vapor-liquid equilibrium is assumed. Physical property data and kinetic data are given in Table1. The kinetic data are shown in Table1.

Following Reyes and Luyben [14], the following process specifications are used.

1. The product flow rate (stream B) from the base of the column is fixed at 0.12 kmol $s^{-1}$.
2. The product purity $x_{B,C}$ is fixed at 0.98 mole fraction $\mathcal{C}$.
3. The reactor exit temperature ($T_{out}$) is limited to 500K at design.
4. The pressure in the reactor is assumed to be 35 bar, and the pressure drop is neglected.

At design, the following assumptions are made.

1. The minimum approach temperature differences for the heat exchangers are fixed at 10 K in HX1 and 25 K in HX2.
2. The reflux drum temperature in the distillation column is fixed at 316 K (to back-calculate column pressure)
3. Distillation columns are designed by setting the total number of trays ($N_T$) equal to twice the minimum number of trays ($N_{min}$) and the optimum feed tray is estimated from the Kirkbride equation.
4. The vapor leaving the vaporizer is at its dew point temperature, given P=35 bar.
5. The ratio of furnace duty to total preheat duty is fixed at 20% ($Q_F/Q_{TOT}$=0.2).
6. The distillate composition of $\mathcal{C}$ is fixed at 1%.

*2.2 Steady-state design and analysis*

With the given specifications, we can complete the steady-state design for any given reactor conversion and reactant distribution. The steady-state conditions of all streams in the ternary recycle system are calculated from balance equations as shown in Appendix A. Next, shortcut methods are applied to find the minimum number of trays (Fenske equation) for distillation columns, locate the feed tray location (Kirkbride equation), and size the column diameter. The heat transfer areas for the reboiler and condenser are also computed from the vapor flow rates.

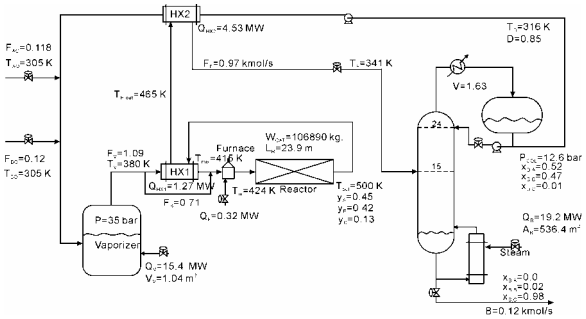

Fig. 1. process flowsheet for the recycle process with optimal design.

Table 1. Physical properties and kinetics data for steady state design

| | component | | |
|---|---|---|---|
| | $\mathcal{A}$ | $\mathcal{B}$ | $\mathcal{C}$ |
| Molecular weight, kg kmol$^{-1}$ | 17.5 | 17.5 | 35 |
| heat of vaporization at 273 K, kJ kmol$^{-1}$ | 16 629 | 16 629 | 16 629 |
| liquid heat capacity, kJ kmol$^{-1}$K$^{-1}$ | 56 | 56 | 112 |
| vapor heat capacity, kJ kmol$^{-1}$K$^{-1}$ | 35 | 35 | 70 |
| Antoine vapour pressure equation constants[a] | | | |
| $A_j$ | 9.2463 | 8.5532 | 7.8600 |
| $B_j$ | -2000 | -2000 | -2000 |
| Heat of reaction, kJ mol$^{-1}$ | -23237 | | |
| Specific reaction rate, kmol$^{-1}$ bar$^{-2}$ kg$_{cat}^{-1}$ | $0.3882e^{6971(6.8.314T}$ | | |

[a] $P_j^s$ in bar and $T$ in Kelvin: $\ln P_j^s = A_j + B_j/T$

*2.2.1 Simplified TAC model.* Following the approach of Malone et al. [15], the TAC model is linearized.

$$\mathrm{TAC} = K_0 + K_1 W_{CAT} + K_2 N_T + K_3 V_S + K_4 Q_F + K_5 Q_V + K_6 V_V + K_7 A_H \quad (1)$$

For the purpose of comparison, it is useful to express the simplified TAC model in terms of process variables, e.g., conversion, reactant distribution, relative volatilities, and reaction rate constant. This can be done by substituting relevant process variables for the equipment size, tray numbers, and vapor rates in Eq.(1). From the mass balance equation, the total amount of catalyst $W_{CAT}$ (implying reactor size, $V_R$) can be expressed as:

$$W_{CAT} = \frac{1}{N_R B P^2 k_o} \sum_{i=N_R}^{1} \frac{F_i^2}{e^{-E/RT_i}\left[\frac{N_R - i}{N_R} + \frac{-\Delta H y_A}{C_P(T-T_o)(1+y_C)}\right]\left[\frac{N_R - i}{N_R} + \frac{-\Delta H y_B}{C_P(T-T_o)(1+y_C)}\right]}$$

where $B$ is the production rate, $N_R$ is no. of lumps in the reactor ($N_R$=50), $F_i$ denotes molar flow rate in each lump, $P$ is pressure in the reactor, $y_A$, $y_B$, $y_C$ are mole fractions in the reactor effluence stream, $-\Delta H$ denotes heat of reaction. Next, we use Fenske equation for the minimum number of trays and set the total number of theoretical trays as $N_T$=2$N_{min}$.

Then the vapor rate can be found from the minimum reflux ratio($V_S = (1.2R_m + 1)D$). And the minimum reflux ratio equation of Glinos and Malone [16] is used.

When the conversion ($y_C$) and reactant distribution ($y_A/y_B$) are given, we can find the TAC immediately.

*2.2.2 Optimal Paths.* The objective here is to find the optimal reactant distribution for different conversion. This locus is termed as optimal TAC trajectory. Consider the following system parameters: production rate $B$ = 0.12 kmol/s, product purity $x_{B,C}$= 0.98, reactor outlet temperature $T_{out}$ = 500 K, $Q_F/Q_{total}$ = 0.2, vaporizer outlet stream temperature $T_V$ = 380 K, column feed temperature $T_F$ = 336 K. For a given $y_C$, the optimal reactant distribution can be found by taking the derivative of the simplified TAC (Eq.(1)). First, we substitute $y_B$ and $y_C$ for $y_A$ in the

cost model and, then, take the derivative with respect to $y_B$. Since the fractional recoveries are fixed and $K_i$'s are constant. Because of $C_{PA}=C_{PB}$, the last four term of Eq.(1) can be eliminated and can be simplified to:

$$\frac{\partial TAC}{\partial y_B} = K_1 \frac{\partial W_{CAT}}{\partial y_B} + K_3 \frac{\partial V}{\partial y_B} \qquad (2)$$

For any given $y_C$, we can find the optimal $y_B$ by solving Eq.(2) and subsequently optimal reactant distribution along the trajectory as shown in Fig. 2. Next the TACs along the trajectory are compared and the true optimum is thus obtained. Fig. 2 reveals the changes of TAC as $y_C$ varies and the minimum TAC corresponds to $y_A$=0.45, $y_B$ =0.42, $y_C$ =0.13 with a TAC of $4.21\times10^7$\$/year. Table 2 gives the steady-state operating conditions for the optimal design. Note that, unlike the isothermal operation, the optimal trajectory does not reach the pure product corner as indicated by the dashed line in Fig. 2. The reason is that the lower-end of reactor inlet temperature is limited by the vaporizer temperature, a constraint imposed by the physical properties of reactants $\mathcal{A}$ and $\mathcal{B}$. The optimal trajectory (Fig. 2) also reveals that, at low conversion, the separation cost dominates and a biased reactant distribution with LK in excess ($y_A/y_B>1$) is preferred, and, as the conversion increasing, the reactor cost becomes more important and an equally distributed reactant ($y_A/y_B=1$) is favored. The tradeoffs between reactor and separation costs are clearly illustrated in Fig. 2 for different values of $y_C$ along the optimal trajectory.

*2.3 Effect of process parameters on optimal path and true optimality*

The analytical expression of Eq.(2) allows us to explore the effects of kinetics parameters and vapour liquid equilibrium on the optimal trajectory and corresponding optimal design. Fig. 2A reveals that as the maximum allowable reactor outlet temperature increases, the optimal trajectory converges to the center line at a larger $y_C$. The reason is that a higher reactor temperature leads to a smaller reactor costs and this, in turn, reduces the relative cost of reactor (compared to the separation cost). Moreover, the reactant distribution becomes biased (light reactant $\mathcal{A}$ in excess) as $T_{out}$ increases.

Next the effects of relative volatilities on the optimal trajectory are examined. Fig. 2B shows that, for fixed reactor outlet temperature, changes in the relative volatility of intermediate key ($\mathcal{B}$) from $\alpha_B$=1.5 to $\alpha_B$=3 do not produce significant difference. Because a larger $\alpha_B$ results in a lesser separation cost and, therefore, the trajectory converges to center line at a lower conversion, but not by much.

If the heat of reaction increases, the optimal trajectory converges faster toward the center line as shown in Fig. 2C. The reason is the reactor inlet temperature will become lower for system with a larger heat of reaction (this can be seen from the overall energy as will be discussed in the next section) and this in turn will lead to a higher reactor cost. This is exactly what Fig. 2C reveals, but the true optimal remains at almost the same reactant distribution.

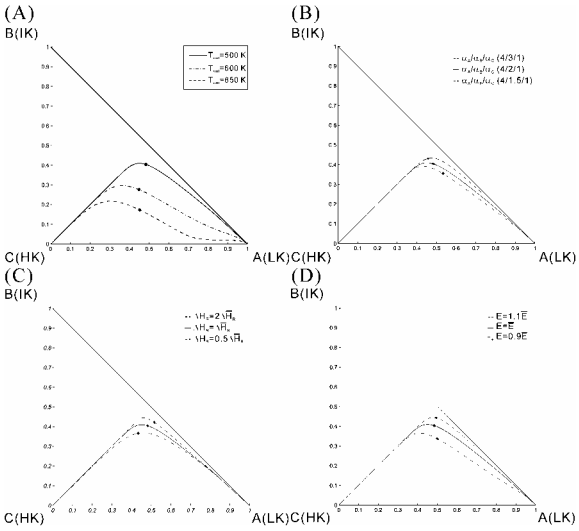


Fig. 2. Optimal TAC trajectory and design for different specifications on (A) reactor outlet temperature, (B) relative volatilities, (C) heat of reaction, (D) activation energy.

It is well known that chemical reactions with large activation energies present difficult control problems because of the rapid increase in the reaction rate as the temperature increases. It also presents difficult reactor temperature control problem when feed-effluent heat exchanger is installed as the result of large reactor gains ($T_{out}/T_{in}$). Fig. 2D shows that, from steady-state economic perspective, the relative reactor cost will be higher for reactions with large activation energy. Therefore, the optimal trajectory converges to the center line at a much lower $y_C$ value and, more importantly, the true optimum is also located closer to the center line which implies equally distributed reactant.

The optimal trajectory can be computed directly from Eq.(2) and this facilitates the investigation of chemical reactions with different kinetics parameters and vapour liquid equilibrium. More importantly, the trajectories obtained provided insight to possible tradeoffs between design and control for different bimolecular reactions.

## 3. OPERABILITY

The material and energy balances provide the basis for steady-state operability analysis [13,17]. For a simple isomerization reaction, the production rate in terms of recycle ratio and subsequently control structure can be devised. Similar approach is taken for the case of adiabatic tubular reactor.

As pointed out earlier, for adiabatic reactor, the temperatures ($T_{in}$ and $T_{out}$) play significant role in operability and energy balance has to be taken into consideration. Without loss of generality, let us use one-lump adiabatic tubular reactor to illustrate the derivation. The relationship between heat generation and the production rate can be expressed as (Luyben, 2001), and it can be derived from reactor energy balance.

The production rate for adiabatic tubular (actually, CSTR) becomes:

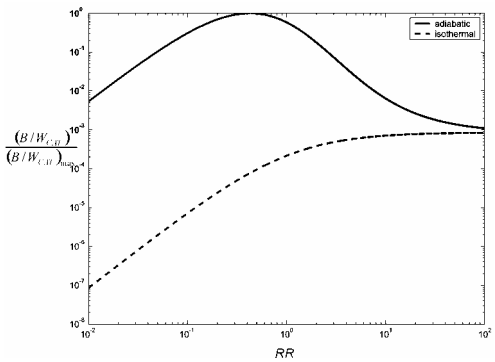


Fig. 3. Normalized production rate as a function of recycle ratio (RR) for adiabatic and isothermal operations.

$$B = W_{cat} k_o P^2 \exp\left( \frac{-E}{R\left( T_{in} + \frac{(-\Delta H)}{(1+RR)C_P} \right)} \right) \frac{x_{D,A} x_{D,B} RR^2}{(1+RR)^2} \quad (3)$$

Comparing Eq.(3) with isothermal system, one immediately observes a significant difference in the reaction rate constant where, for the case of adiabatic tubular, it is a function of recycle ratio (*RR*). Also shown in Eq.(3) is that the reactor inlet temperature ($T_{in}$), the reactor pressure (*P*), and the distribution of the reactant ($x_{DA}/x_{DB}$) also play visible roles in the production rate expression.

Insights can be gained by examining Eq.(3). Let us explore the effects of different design/operating variables on the production rate changes.

*3.1 Recycle Rates (RR=D/B)*

Let use kinetics data and reactant distribution of the optional design to illustrate the difference between isothermal and adiabatic operation. That is: $T_{in}$ = 424 K, *P* = 35 bar, and $x_{DA}/x_{DB}$ = 0.52/0.47. The normalized production per kg of catalyst, $B/W_{CAT}$, can be computed as the recycle ratio (*RR*) changes. Fig. 3 shows a non-monotonic behavior for a wide-range of recycle ratio. At low *RR* (corresponding to high conversion or large $y_C$), the production rate increases as we increase *RR*. However, the opposite behavior is observed at high *RR* region (low conversion). That is $B/W_{CAT}$ decreases with an increase in RR and this is the typical results as seen in many of Luyben and co-worker examples. The reason for that is the temperature effect ($T_{out}$ of the reactor) dominates the concentration effect (at high *RR* region). In other words, a smaller production rate will result for an increase in *RR* for an adiabatic reactor at low conversion with high activation energy (*E*) and high heat of reaction (-*ΔH*). This can be quantified by taking the derivative of Eq.(3) with respect to *RR*. After some algebraic manipulation, we have:

$$\left( \frac{\partial B / \bar{B}}{\partial RR / \overline{RR}} \right)_{P,W_{cat},y_A,y_B} = \frac{2}{1+\overline{RR}} - \frac{E}{R\bar{T}_{in}^{\,2}} \frac{\left(\bar{T}_{out} - T_{in}\right)\overline{RR}}{1+\overline{RR}} \quad (4)$$

Eq.(3) clearly indicates the competing effect between concentration and temperature. Note that, for isothermal operation, i.e., $T_{reactor}=T_{in}$, we have only the concentration effect. That is:

$$\left( \frac{\partial B / \bar{B}}{\partial RR / \overline{RR}} \right)_{P,W_{CAT},y_A,y_B} = \frac{2}{1+\overline{RR}} \quad (5)$$

Fig. 3 also shows the production rate variation for isothermal operation and the "snowball effect" is also evident at high *RR* region.

*3.2 Reactor Inlet Temperature ($T_{in}$)*

The reaction inlet temperature is an ideal candidate for the throughput manipulator (TPM) and this is especially true for reaction system with high activation energy where the *RR* is relatively ineffective. Again, the sensitivity of the production rate for a change in $T_{in}$ can be derived from Eq.(3). If the reactant distribution is maintained at the nominal value, we have:

$$\left( \frac{\partial B}{\partial T_{out}} \right)_{P,W_{CAT},y_A,y_B} = \frac{\bar{B}EK_R}{R\bar{T}_{out}^{\,2}} \quad (6)$$

Eq.(6) clearly shows that from steady-state viewpoint. $T_{in}$ is a good TPM for systems with large E. Compared to the isothermal CSTR case, the sensitivity is amplified by the reactor gain $K_R$ which is the sensitivity between the inlet and outlet temperature (i.e., $K_R=\partial T_{out}/\partial T_{in}$). As pointed out by Chen and Yu [11, 12], a heat integrated reactor via feed-effluent heat exchanger can easily become open-loop unstable for system with a high reactor gain ($K_R$). Therefore, controllability problem may arise when we try to recover more heat form the hot gas of the reactor effluent. Nevertheless, Eq.(6) indeed shows that $T_{in}$ is a good candidate for TPM.

*3.3 Reactor Pressure (P)*

In theory, the reactor holdup is also a good candidate in handling production rate changes. And, for the case of isothermal operation, this forms the basis to overcome "snowball effect" as pointed out by Wu and Yu [18]. The problem handling capability can be quantified the taking the derivative of Eq.(3) with respect to the pressure. Thus, one obtains:

$$\left( \frac{\partial B}{\partial P} \right)_{T,W_{CAT},y_A,y_B} = \frac{2\bar{B}}{\bar{P}} \quad (7)$$

Steady-state analysis clearly shows the reactor pressure is a good choice for TPM. However, for gas-phase reactor, interaction between pressure and temperature may lead to dynamic problem. The thermal inertia may cause significant variation in the reactor inlet temperature unless a large gas-phase holdup is employed.

*3.4 Reactant Distribution*

Before heaving this section, we would like to look at an important design parameter: reactant distribution ($y_A/y_B$). The reactant distribution in some cases represents an important tradeoff between design and control as shown in the case 2 Reyes and Luyben [14] where we have a bimolecular reaction with high activation energy. The optimal TAC corresponds to an almost equally distributed reactant distribution, but the operability consideration lead to a biased reactant distribution (e.g., one of the reactant is in excess). Let us consider the case where the reactant $\mathcal{A}$ is in excess. The sensitivity in the

production rate variation for changes in $y_B$ can be expressed as:

(A)

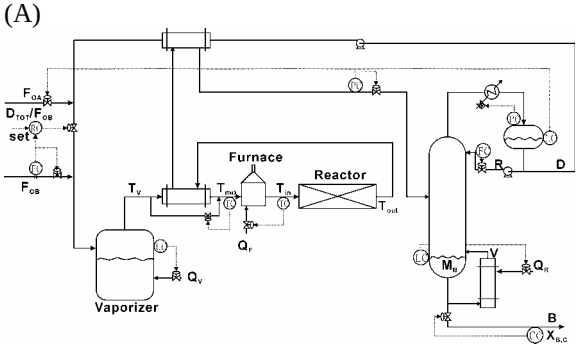


(B)

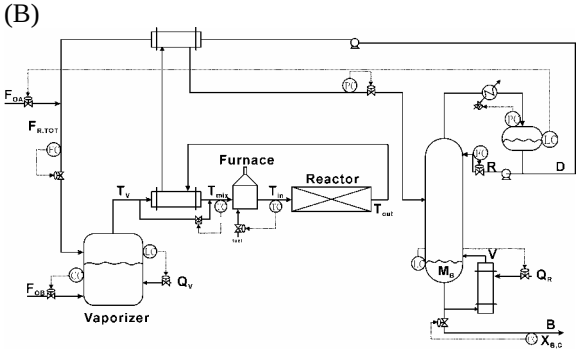


Fig. 4. Control structure fixing (A) recycle ratio (CS1) and (B) reactor exit composition (CS2).

$$\left(\frac{\partial B/\bar{B}}{\partial y_B/y_B}\right)_{P,W_{CAT},T_{in},RR} = \frac{(y_A - y_B)}{y_A} \qquad (8)$$

It clearly shows that, a small change in the limiting reactant $\mathcal{B}$ can lead to significant change in the production rate and this is especially true when $\mathcal{A}$ is in large excess.

## 4. CONTROL

### *4.1 Control Structures*

The on-going analysis provides the basis for control structure design. Two scenarios are considered. One is the optimal design as shown in Table 2 where we have a case of almost equally distributed reactant and the other case corresponds to a biased reactant distribution (also shown in Table 2). Two control structures are devised for these two cases. In the first case, the recycle ratio is fixed as shown in Fig. 4A, denoted as CS1 hereafter, and in the second case the reactant distribution is maintained by controlling one of the reactant in the vaporizer, called CS2 hereafter (Fig. 4B).

Fig. 4 shows the essential loops for these two control structures.

### *4.2 Throughput Manipulator*

As mentioned in section 3, we have three candidate throughput manipulators. One is the reactor inlet temperature ($T_{in}$) which is denoted as CSia, the second one is the reactor pressure (P) which is called CSib, and the third one is the recycle flow rate which is the control structure CSic. Nonlinear dynamic simulations were performed to evaluate the effectiveness of different control structures. The modeling approach of Reyes and Luyben [19] was taken and the nonlinear recycle plant was solved numerically using FORTRAN. Two different designs are tested.

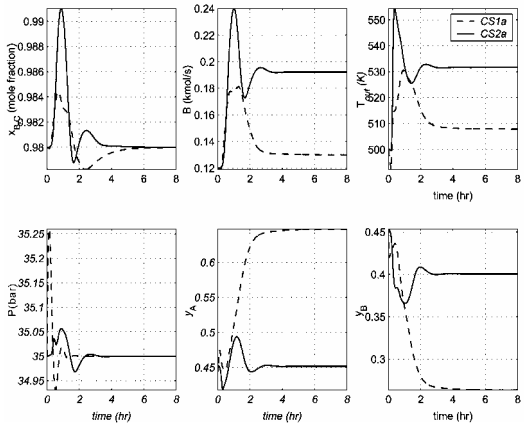


Fig. 5. Closed-loop performance using CS1 and CS2 for $\Delta T_{in}$ = +5 K (case 1).

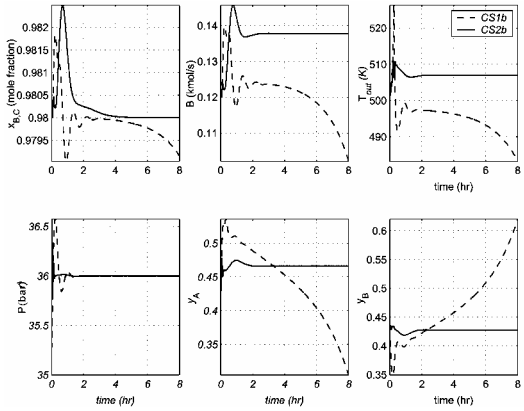


Fig. 6. Closed-loop performance using CS1 and CS2 for $\Delta P$ = +1 bar (case 1).

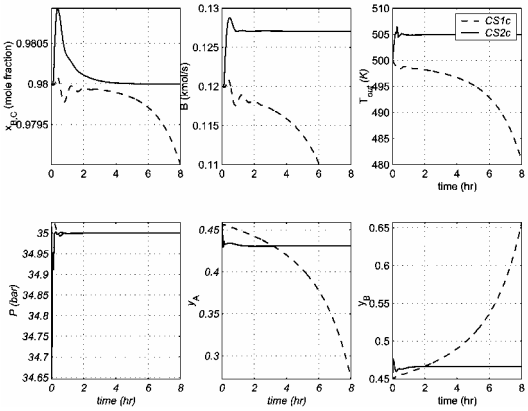


Fig. 7. Closed-loop performance using CS1 and CS2 for $\Delta D$ = +5 % (case 1).

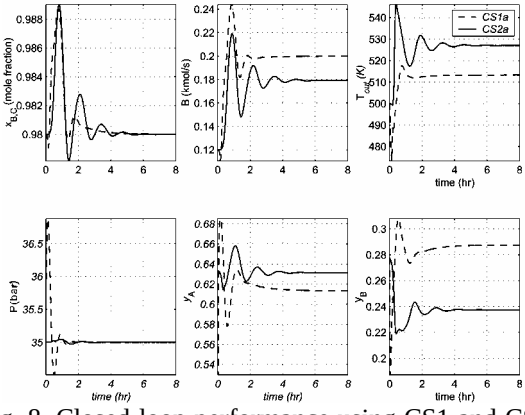


Fig. 8. Closed-loop performance using CS1 and CS2 for $\Delta T_{in}$ = +5 K (case 2).

One is the optimal design (Table 2) which represents the case of almost equally distributed reactant (e.g., $y_A/y_B \approx 1$) and the other case explores the scenario of biased reactant distribution (e.g., $y_A/y_B=2.3$). Let us compare the control performance of CS1 and CS2 for the case of equally distributed reactants. Fig. 5 shows the production rate changes for a +5 K increase in $T_{in}$. Despite quite similar process dynamics (e.g., settled in 4 hours), different magnitudes in production rate changes are observed. For CS2, it results in 61% production increase while, for CS1, only 8.3% production rate increased can be achieved. The reason for the smaller magnitude in production rate increase for CS2 is that the effect of $T_{in}$ is offset by the re-distribution reactant as shown in Fig. 5. This was not seen for CS1 become the composition of B is controlled to maintain the optional reactant distribution. Similar results can also seen when the reactor pressure and recycle flow are used as TPM. Also notice that significant change in $T_{out}$ can be seen for CS1 when $T_{in}$ is used as TPM and this may lead to potential problem in practice.

Finally, for the case when $\mathcal{A}$ is in excess (e.g., $y_A/y_B=2.3$), exactly the opposite results were obtained when comparing CS1 and CS2 (Fig. 4). Again, for a +5 K change in $T_{in}$, a larger production rate increase can be achieved using CS2 (50%) as compared ti that of CS1 (67%) while having a lower $T_{out}$ as shown in Fig. 8. The reason is obvious that the redistribution of reactants contributes to the production rate increase.

## 5. CONCLUSION

In this work, recycle process with the bimolecular reaction, $\mathcal{A}+\mathcal{B}\rightarrow\mathcal{C}$, is investigated. The total annual cost (TAC) is used to evaluate economic incentive for different designs. The simplified TAC facilitates the search for optimal reactant distribution under conversion. Similar to isothermal CSTR case, the optimal TAC trajectory starts form the light reactant corner at low conversion (where the separation cost dominated) toward the equally distributed reactant at a higher conversion (where the reactor cost dominated). Optimal design can thus be computed given different kinetics and relative volatilities provided with cost data. Next, the connection between total production and reactor temperature is derived analytically. It clearly shows the difference between adiabatic and isothermal operation. Moreover, the capability in handling production rate changes can be evaluated. Subsequently, control structures are devised. The results indicate that different control structures should be applied when the optimal reactor composition varies. More importantly, the results show that insight to the recycle process with adiabatic tubular reactor can be gained form fundamental material and energy balances.

## REFERENCES


[1] Gilliland, E. R.; Gould, Boyle, L. A.; (1964) T. J. Proc. Joint Automatic Control Conference, pp 140.

[2] Verykios, X. E. and Luyben, W. L. (1978). Steady-State Sensitivity and Dynamics of a Reactor/Distillation column System with Recycle, **17**, pp. 31, ISA Transactions.

[3] Luyben, W. L. (1994). Snowball Effect in Reactor/Separator Process with Recycle. **33**, pp. 299, Ind. Eng. Chem. Res.

[4] Georgakis, C. (1986). On the Use of Extensive Variables in Process Dynamics and Control, **41**, pp. 1471, Chem. Eng. Sci..

[5] Vinson, D. R. and Georgakis, C. (2000). A New Measure of Process Output Controllability, **10**, pp. 185, J. Process Control.

[6] Luyben, W. L.; Tyreus, B. D.; Luyben, M. L. (1999) Plantwide Process Control, McGraw-Hill, New York.

[7] Yi, C. K. and Luyben, W. L. (1995), Evaluation of plant-wide control structures by steady-state disturbance sensitivity analysis, **34**, pp. 2393, Ind. Eng. Chem. Res..

[8] Semino, D.; Giuliani, G. (1997), Control Configuration Selection in Recycle Systems by Steady State Analysis, **21** , Suppl. S273, Computers Chem. Engng..

[9] Elliott, T. R.; Luyben, W. L. (1995), A Capacity-base Economic Approach for the Quantitative Assessment of Process Controllability during the Conceptual Design Phase , **34**, pp. 3907, Ind. Eng. Chem. Res.

[10] Luyben, M. L.; Tyreus, B. D.; Luyben, W. L. (1996), Analysis of Control Structures for Reaction/Separation/Recycle Processes with Second-Order Reactions, **35**, pp. 758, Ind. Eng. Chem. Res.

[11] Chen, Y. H. and Yu, C. C. (2000), Interaction between Thermodynamic Efficiency and Dynamic Controllability: Heat-Integrated Reactor, **23**, pp. 1077, Comput. Chem. Eng.

[12] Chen, Y. H. and Yu, C. C. (2003), Design and Control of Heat-Integrated Reactors, (in press) , Ind. Eng. Chem. Res..

[13] Cheng, Y. C. and Yu, C. C. (2003) Optimal Region for Design and Control of Ternary Systems, **49**, pp. 682, AIChE J.

[14] Reyes, F. and Luyben, W. L. (2001) Design and Control of a Gas-Phase Adiabatic Tubular Reactor Process with Liquid Recycle, **40**, pp. 3762, Ind. Eng. Chem. Res.

[15] Malone, M. F.; Marquez, F. E.; Douglas, J. M.; Glinos, K. (1985), simple, analytical criteria for the sequencing of distillation columns, **31**, pp. 683, AIChE J.

[16] Malone, M. F.; Glinos, K.; Marquez, F. E.; Douglas, J. M. (1985), Simple, Analytical Criteria for the Sequencing of Distillation Columns, **31**, pp. 683, AIChE J.

[17] Wu, K. L.; Yu, C. C.; Luyben, W. L.; Skogestad, S. (2003), Reactor/Separator Processes with Recycle-2. Design for Composition Control, **27**, pp. 421, Computers Chem. Engng.

[18] Wu, K. L. and Yu, C. C.(1996), Reactor/Separator Processes with Recycle-1. Candidate Control Structure for Operability, **20**, pp. 1291, Computers Chem. Engng.

[19] Reyes, F. and Luyben, W. L. (2001) Extension of the Simultaneous Design of Gas-Phase Adiabatic Tubular Reactor Systems with Gas Recycles, **40**, pp. 635, Ind. Eng. Chem. Res.